🔓 OPEN ACCESS

Single-cell resolution of intestinal regeneration in pythons without crypts illuminates conserved vertebrate regenerative mechanisms

Aundrea K. Westfall[a,b], Siddharth S. Gopalan[a] (ID), Jarren C. Kay[c] (ID), Trevor S. Tippetts[b], Margaret B. Cervantes[b] (ID), Kimberly Lackey[c] (ID), Saiful M. Chowdhury[d] (ID), Mark W. Pellegrino[a] (ID), and Todd A. Castoe[a,1]

Affiliations are included on p. 10.

Canonical models of intestinal regeneration emphasize the critical role of the crypt stem cell niche to generate enterocytes that migrate to villus ends. Burmese pythons possess extreme intestinal regenerative capacity yet lack crypts, thus providing opportunities to identify noncanonical but potentially conserved mechanisms that expand our understanding of regenerative capacity in vertebrates, including humans. Here, we leverage single-nucleus RNA sequencing of fasted and postprandial python small intestine to identify the signaling pathways and cell–cell interactions underlying the python's regenerative response. We find that python intestinal regeneration entails the activation of multiple conserved mechanisms of growth and stress response, including core lipid metabolism pathways and the unfolded protein response in intestinal enterocytes. Our single-cell resolution highlights extensive heterogeneity in mesenchymal cell population signaling and intercellular communication that directs major tissue restructuring and the shift out of a dormant fasted state by activating both embryonic developmental and wound healing pathways. We also identify distinct roles of BEST4+ enterocytes in coordinating key regenerative transitions via NOTCH signaling. Python intestinal regeneration shares key signaling features and molecules with mammalian gastric bypass, indicating that conserved regenerative programs are common to both. Our findings provide different insights into cooperative and conserved regenerative programs and intercellular interactions in vertebrates independent of crypts which have been otherwise obscured in model species where temporal phases of generative growth are limited to embryonic development or recovery from injury.

BEST4+ cells | lipid metabolism | NOTCH signaling | RYGB | stress response

Some degree of intestinal regeneration and renewal is common across vertebrates, including humans, and is best understood in birds and mammals in which intestinal stem cells (ISCs) originating from crypts migrate and differentiate into mature enterocytes (1). Emerging models of small intestine development and self-renewal emphasize the organ's ability to integrate complex signaling pathways and mechanical forces to direct differentiation, maintain homeostasis, and promote function (2, 3). In an extreme example of vertebrate adaptive intestinal regenerative capacity, snakes like the Burmese python (*Python molurus*) undergo months-long fasts, during which time their intestine atrophies to a pseudostratified layer (4). Within 48 h of feeding, their small intestine wet mass doubles, intestinal microvillus length increases fivefold, and their rate of oxygen consumption increases 44-fold (4–9). These extreme phenotypic shifts return back to states similar to the fasted condition by 14 days postfeeding (dpf) (9), and gene expression returns to levels similar to fasted by 10 dpf (8). Despite this extreme regenerative capacity, pythons lack the heterogenous crypt–villus structure that typifies mammalian intestinal regeneration (7), making them a valuable model for understanding conserved yet noncanonical mechanisms underlying vertebrate intestinal regenerative capacity.

Outside of snakes, few vertebrate examples of extreme intestinal regenerative capacity exist in nature, such as hibernating mammals that undergo exaggerated cycles of atrophy and regrowth (10). Despite this rarity, extreme human intestinal restructuring and differentiation has been shown to accompany major surgical intervention: Roux-en-Y gastric bypass (RYGB) reroutes digestion past the human duodenum and causes regenerative transformation and redifferentiation of jejunal architecture and metabolism, which can lead to type 2 diabetes remission (11, 12). Indeed, these findings have prompted interest in human intestinal regenerative capacity and reinforced the emerging view of the small intestine as a major center regulating glucose metabolism and homeostasis (13).

Significance

The vertebrate intestine is well known for its regenerative capacity, but existing research emphasizes the role of a crypt–villus axis in the constant turnover of the intestinal epithelium. Mechanisms that support large-scale intestinal regeneration are poorly understood despite being of major interest to human health. We implement bulk and single-cell RNA sequencing to identify heterogeneity and signaling regimes that drive extensive regeneration in large pythons when breaking a fast. Critical signaling events in python intestinal regeneration mimic embryonic intestinal development, wound healing mechanisms, and human intestinal regeneration after gastric bypass surgery. This suggests that key conserved mechanisms underlie vertebrate intestinal regeneration despite extensive structural and physiological adaptation.

Furthermore, villus atrophy, the inability to regenerate villi, is associated with severe gastrointestinal conditions such as celiac disease in humans (14), and mechanisms to promote regeneration after villus and crypt loss following chemotherapy and radiation are of major biomedical interest (15–17).

In contrast to mammalian systems, heavy-bodied snakes, including pythons, undergo cyclic extreme atrophy and regeneration naturally throughout their lifetime without priming, recovery, or pathological dysregulation (18). Prior work on snake intestinal regeneration has integrated multiple tissue-level "-omics" data types to identify regulatory interactions between conserved stress response, growth, and metabolic pathways that enable a rapid regeneration response (Fig. 1*A*) (8, 19–23). To date, many of the core mechanisms identified in snake intestinal regeneration recapitulate growth and regeneration programs otherwise well understood from mammalian models (24–26), despite the lack of crypts (and thus a crypt–villus axis) in pythons. For example, the NRF2-mediated antioxidant pathway has been linked to python intestinal regeneration and is also known to promote human intestinal regeneration after

radiation therapy (17, 21). Taken together, this raises questions about the mechanisms of regenerative signaling in snake intestines and the degree to which these mechanisms may be conserved in vertebrates. Accordingly, pythons represent an attractive alternative vertebrate model that may provide distinct insights into conserved modes and mechanisms of intestinal regeneration and differentiation independent of the canonical mammalian crypt–villus axis.

Here, we combine single-nucleus RNA sequencing (snRNAseq) with tissue-level mRNAseq from Burmese python proximal small intestine at fasted and multiple postprandial timepoints to characterize tissue-wide and cell type-specific temporal responses to fasting and feeding. We first compare regenerative responses in pythons to broad regenerative mechanisms proposed in prior studies based on a different snake species, and identify core conserved regenerative programs associated with snake intestinal regeneration using tissue-level mRNAseq (8, 21–23). We then integrate single-nucleus RNAseq in pythons to investigate how these core regenerative programs manifest in distinct temporal and cell type-specific ways throughout the regenerative process and infer
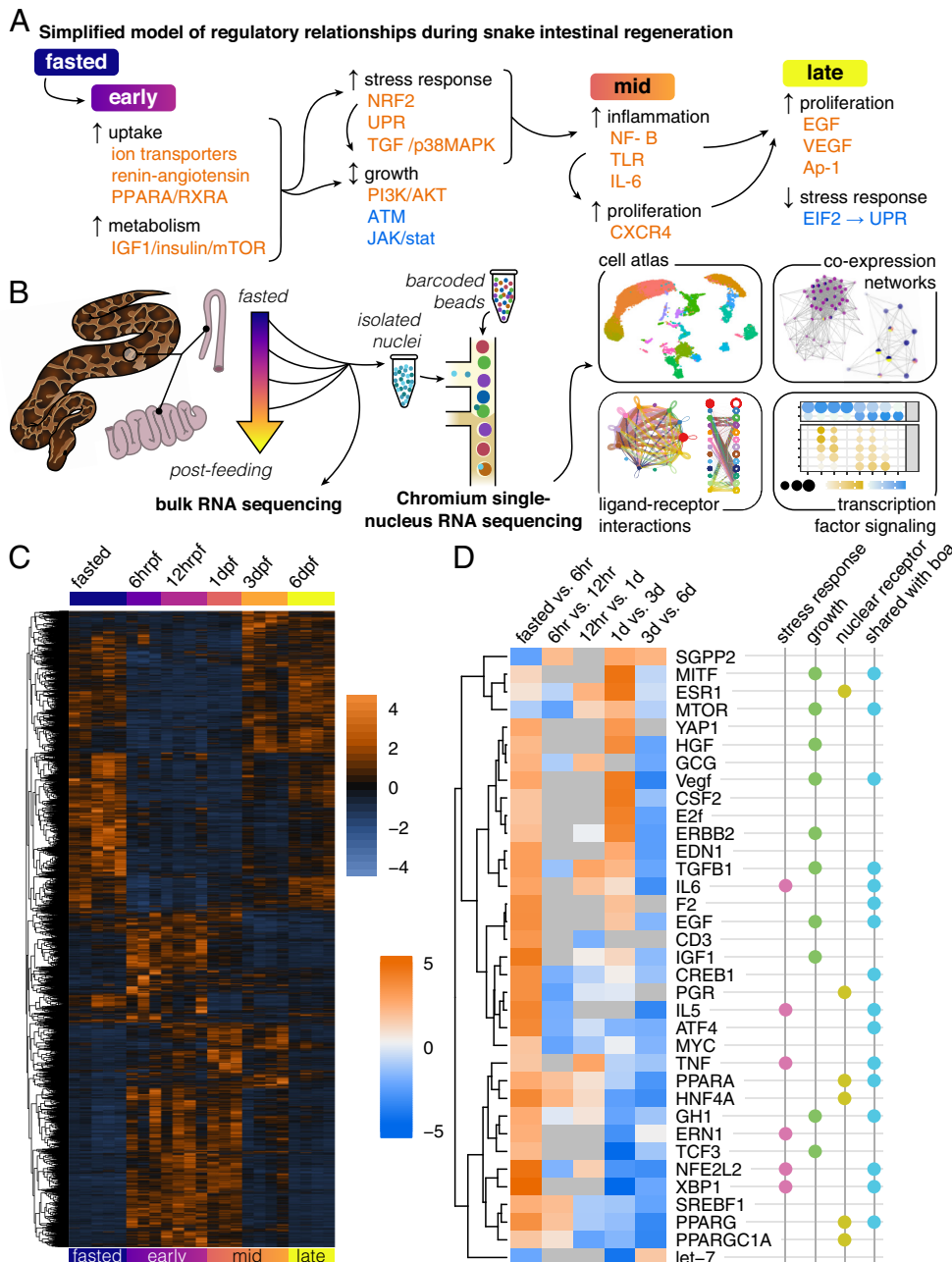

Fig. 1. Intestinal regeneration in the python broadly recapitulates known models. (*A*) Overview of hypothesized model for snake intestinal regeneration. Orange indicates upregulated upstream regulatory molecules and blue indicates downregulated. (*B*) Overview of experimental design. (*C*) Heatmap of significant differentially expressed genes in the bulk RNAseq. (*D*) Activation of top 35 URMs with significant activation in multiple timepoints from IPA over the course of the time series, hierarchically clustered. Functional annotations indicate major stress response and inflammation regulators, growth factors or regulatory molecules, and nuclear receptors as well as whether the URM was shared with the boa constrictor. UPR, unfolded protein response.

the roles of distinct cell populations in intercellular signaling linked to regenerative reprogramming. Finally, we compare regenerative responses in pythons to those induced by human RYGB to identify shared signaling mechanisms common to both python and human intestinal regeneration and redifferentiation. Our findings collectively highlight unique evidence for the existence of cellular and intercellular intestinal regenerative signaling mechanisms that are conserved across vertebrates with broad relevance to human disease and regeneration.

Results

Conserved Intestinal Regenerative Signaling in Heavy-Bodied Snakes. Prior tissue-level studies on a different snake species (*Boa constrictor*) (22) have led to a proposed model for the time course of activation of pathways and processes underlying postfeeding intestinal regeneration in snakes (Fig. 1*A*). Tissue-level mRNAseq data from Burmese pythons (Fig. 1*B*) was mapped to the python reference genome (27) that contains 22,541 annotated genes, and 19,713 of these were detected by our RNAseq data. These data revealed thousands of differentially expressed genes within the first day following feeding (Fig. 1*C*). Consistent with prior studies that suggest gene expression programs reset to fasted levels around 10 dpf) (8, 9), our 6 dpf sampling shows gene expression is already converging back toward fasted states (Fig. 1*C*). Based on these tissue-level data, we used Ingenuity Pathway Analysis (IPA) (Qiagen Inc.) to infer activation of upstream regulatory molecules (URMs) and mechanistic networks, which confirm that Burmese pythons and boa constrictors exhibit shared patterns of URM activation at early timepoints, such as of *NFE2L2*, *XBP1*, *ATF4*, *TGFB1*, *PPARA*, and *CREB1* (Fig. 1*D*) (22). For example, consistent with the proposed model (Fig. 1*A*) and with prior inferences of URMs activated in boa constrictors (22), our URM analyses (Fig. 1*D*) identify early activation of mTOR (URMs: MTOR) and PPAR signaling (URMs: PPARG and PPARA), along with stress responses (URMs: ATF4, XBP1, NFE2L2, IL6) and additional late stage growth signaling (URMs: EGF and Vegf) that coincides with the decline of stress response signaling (Fig. 1*D*). These similarities between distinct snake species also agree with prior conclusions that multiple species of snakes share a core set of intestinal regenerative signaling mechanisms that include the coordinated activity of growth and stress responses in coordinating early regenerative growth (Fig. 1*A*) (23).

Regeneration and Epithelial Heterogeneity Despite the Absence of Crypts. To determine cell-type-specific contributions to python regenerative growth, we generated snRNAseq of proximal small intestine samples from Burmese pythons at fasted, 6 hours postfeeding (hrpf), 12 hrpf, and 1 dpf. This resolved 21,109 high-quality single-cell inferences with a median of 878 genes per cell, a mean of 51,937 reads per cell, a median of 1,174 unique molecule identifier counts per cell, and a total of 19,182 genes expressed. These cells were clustered and assigned to cell types based on the expression of canonical intestinal cell markers (Fig. 2 *A–D* and *SI Appendix,* Fig. S1) (28–31). We identify most major cell types from the epithelial monolayer and surrounding connective tissue, consisting of smooth muscle, stromal cells, and fibroblasts that share a mesenchymal origin (29). Nonepithelial cell types (such as endothelial and hematopoietic cells) and secretory epithelial cell types (such as goblet cells) form singular clusters regardless of timepoint, while absorptive cells tend to cluster separately by their point in the time series, suggesting that the absorptive cells undergo more substantial shifts in gene expression upon feeding (Fig. 2 *A* and *B*). Based on our snRNAseq data, we compared the relative frequencies of distinct cell types across time

points (*SI Appendix,* Fig. S2) and found that the relative frequencies of multiple epithelial cell types vary across time points and that goblet cells in particular appear to expand in relative frequency from the fasted to 1 dpf timepoint.

No cluster of cells expresses markers consistent with crypt-localized ISCs or Paneth cells (Fig. 2*D* and *SI Appendix,* Fig. S1), although a population of 1dpf-exclusive mesenchymal cells exhibits high expression of some stemness markers. Also consistent with a lack of crypts in pythons, neither stromal cells nor lymphatic endothelial cells express *RSPO3*—essential to the survival and expansion of the crypt ISC niche (32)—although other mesenchymal cell types have high *RSPO3* expression (Fig. 2*D*). The expression level and relative fraction of cells with any expression of these markers are both stable across postfeeding time points (*SI Appendix,* Fig. S3). Collectively, these data support the absence of a structured crypt in the python intestine responsible for directing regeneration in other vertebrate systems.

Distinct Mesenchymal Cell Responses Direct Phases of Intestinal Restructuring. Recent work in mammalian systems has established roles of distinct mesenchymal cell populations in directing early embryonic villus development and promoting regeneration in mammalian crypts (2, 33). Considering these findings, and the extreme intestinal regenerative capacity of pythons in the absence of crypts, we investigated cell-type-specific cell–cell signaling during early phases of the python regenerative response. At 6 hrpf, the strongest intercellular signaling occurs from fibroblasts to smooth muscle; bidirectionally among smooth muscle, stromal, and submucosal cells and from mesenchyme to endothelia (Fig. 3*A* and *SI Appendix,* Fig. S4). Most ligands expressed among mesenchymal cells are extracellular matrix (ECM) proteins (nonfibrillar collagen types IV and VI, *FN1*) interacting with cell–ECM adhesion receptors (*ITGA1*/*ITGA9* and *ITGB1*), although ligand–receptor pairs involving smooth muscle cells also include laminins, key proteins of the basement membrane (Fig. 3*B*). These intercellular signaling patterns recapitulate ECM and adhesion dynamics measured in the first wave of villus morphogenesis, during which time-specific PDGFRA^{high} stromal cells aggregate to initiate villus extension (34). Python intestinal regeneration exhibits an expansion of PDGFRA^{high} stromal cells (Fig. 3*C*), which differentially express genes such as collagen types IV and VII subunits (*COL4A5*, *COL4A6,* and *COL7A1*), neuregulin-1 (*NRG1*), and *DLL1*, while PDGFRA^{low} fibroblasts express high amounts of *CYR61* and *ZEB2* (Fig. 3*D*). High nonfibrillar collagen expression is consistent with PDGFRA^{high} embryonic mesenchyme, while *NRG1* is robustly expressed by intestinal mesenchyme to promote fetal-like stem cell proliferation and regeneration after damage (35). However, *DLL1* and *CYR61* are expressed at the intestinal crypts to promote proliferation, a role that might be instead assumed by mesenchymal cells in the python (36, 37). Overall, these results suggest that early python intestinal regeneration involves the joint activation of pseudoembryonic restructuring and canonical wound healing mechanisms in the intestinal mesenchymal niche to promote villus growth.

Distinct Epithelial Cell Lineages Follow Distinct Trajectories during Regeneration. While the mesenchymal cell populations are critical to early regeneration, epithelial cells comprise the majority of intestinal cells and exhibit extensive heterogeneity and multiple distinct trajectories of responses throughout python regeneration. To understand the relevance of these distinct profiles,
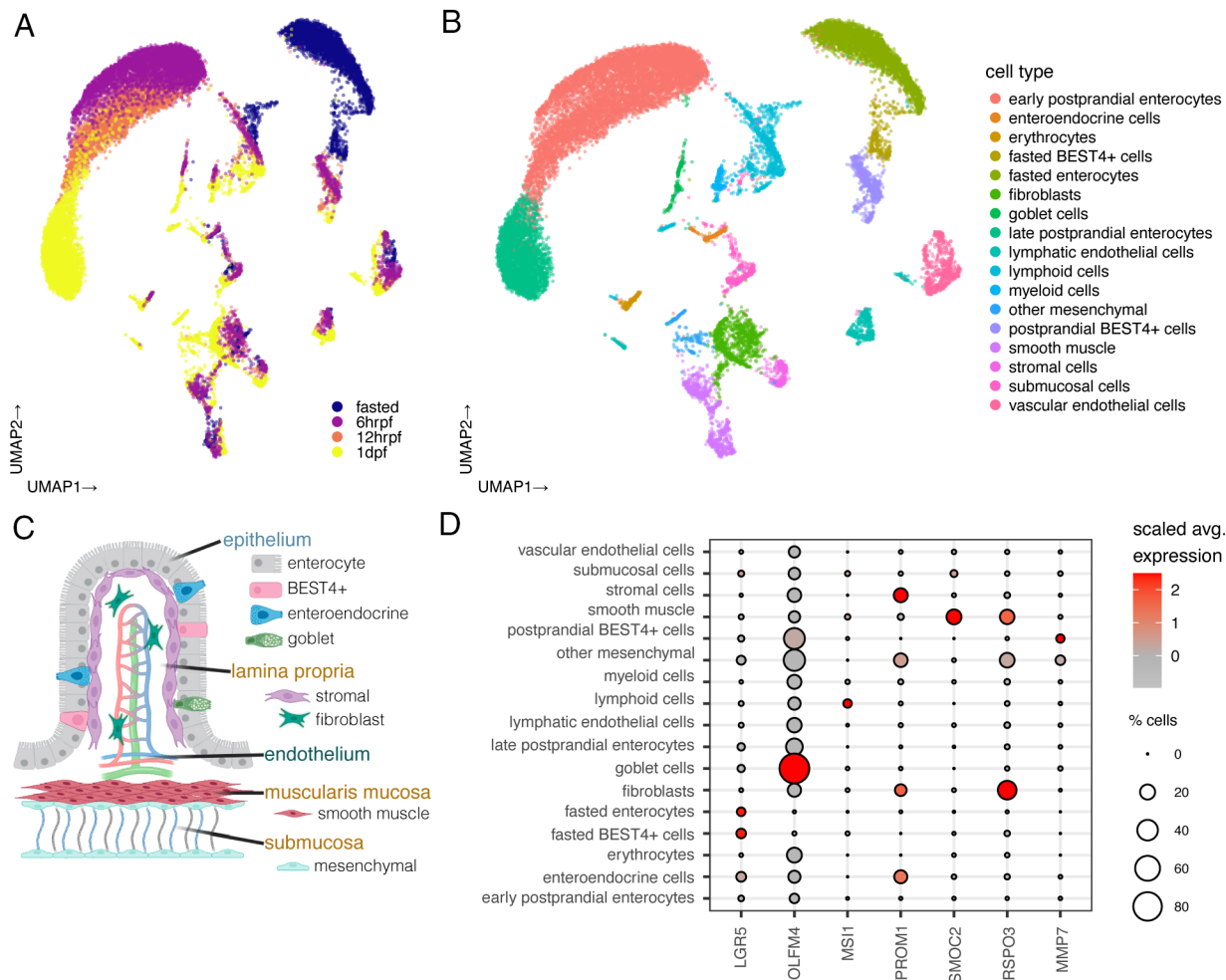
Fig. 2. Absence of a stem cell niche in the python small intestine. (*A*) UMAP visualizations of samples from four time points and (*B*) major cell types. (*C*) Overview of intestinal epithelial cell types and major neighboring tissue layers. Created with BioRender.com. (*D*) Expression of stem cell and crypt niche markers in python cell types. Although some cells express stem cell markers, there is no distinct cluster of crypt stem cells as seen in mammalian tissue.

we characterized these shifts for two distinct absorptive epithelial cell lineages: enterocytes and recently characterized BEST4+ cells (Fig. 4 *A* and *B* and *SI Appendix*, Fig. S5). Over the postfeeding time course from fasted to 1 dpf, python enterocytes exhibit changes in metabolic programs, insulin responsiveness, and activation of PPAR signaling and fatty acid metabolism after feeding, while BEST4+ cells undergo signaling shifts associated with hormone secretion, inflammatory regulation, and nerve synapses (*SI Appendix*, Fig. S4). These results highlight that enterocytes and BEST4+ cells diverge on two distinct trajectories during early regenerative signaling in response to key differential signaling inputs of nutrient sensing (in enterocytes) vs. systemic and neuronal inputs (BEST4+) that affect downstream function and activation of these distinct cell populations.

Enterocytes Integrate Stress Response and Lipid Metabolism. To identify signaling programs shared among enterocytes at different regenerative stages, we used gene–gene correlations to infer coexpression network modules that characterize the core gene expression programs among cell populations. Across all cells, the two largest and most highly expressed gene modules are enriched in epithelial cell types and centered on the genes *APOA4* and *CHOP/DDIT3* (hereafter *DDIT3*), respectively (Fig. 4 *C*–*E* and *SI Appendix*, Figs. S6 and S7). The *APOA4* network module is expressed among all postprandial enterocytes, and pathway enrichment of the genes in the *APOA4*

network highlights central roles of fatty acid metabolism, digestion, biosynthesis, and transport, with key links to *PPARA* and retinoids (Fig. 4*E*). The two most central genes to the network (other than *APOA4*) are *RBP2*, typically highly abundant in the small intestine epithelium, and *FABP2*, considered a classical enterocyte marker. Both of these are only expressed in postprandial python epithelial cells and are not observed in fasted epithelial cells (*SI Appendix*, Fig. S8). *APOA4*, alongside *FABP2* and other apolipoproteins, have zonate expression in mammalian villi and are expressed at villus tips (38), and the contrast of their absence in fasted enterocytes against high postfeeding expression is consistent with mesenchymal expression that indicates extreme growth and extension of villi. In contrast, the DDIT3 module is primarily present in 1 dpf enterocytes and shares 29 genes with the APOA4 module, including *BMP1*, *HIF1A*, *PIK3C2A*, and *CREB3*. While DDIT3 plays well-known roles in the unfolded protein response (UPR) and apoptosis, we also find that the DDIT3 module is specifically enriched for genes involved in lipid metabolism and biosynthesis (Fig. 4 *D* and *E*). These results provide evidence for a noncanonical role of DDIT3 in regenerative growth through its interactions with lipid metabolism.

BEST4+ Cells Coordinate Lymphatic Regeneration via NOTCH Signaling. The roles of BEST4+ cells in the GI tract are poorly understood. Our single-cell data identified a population of these cells in the python intestine, which was confirmed by BEST4
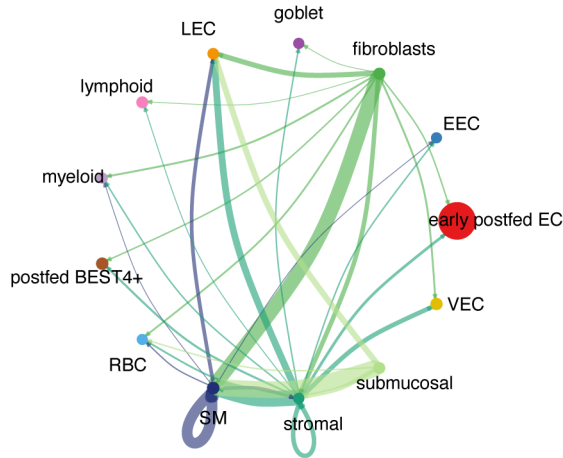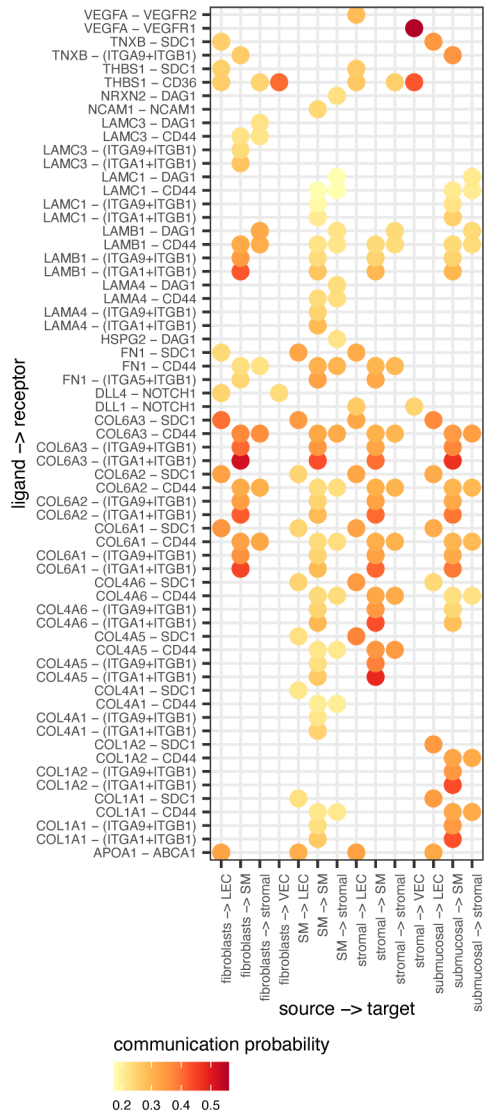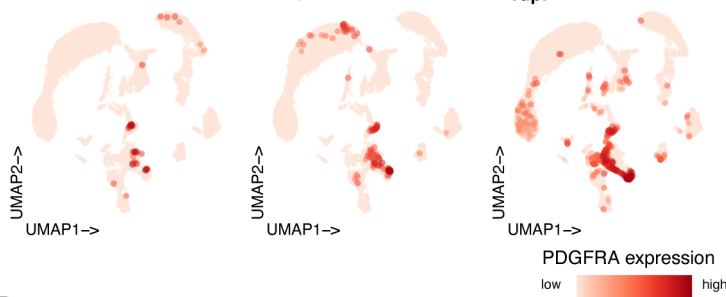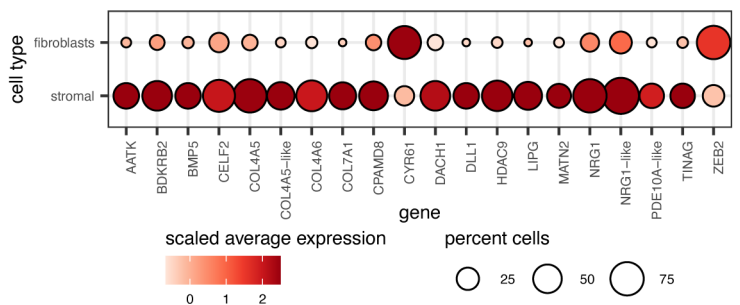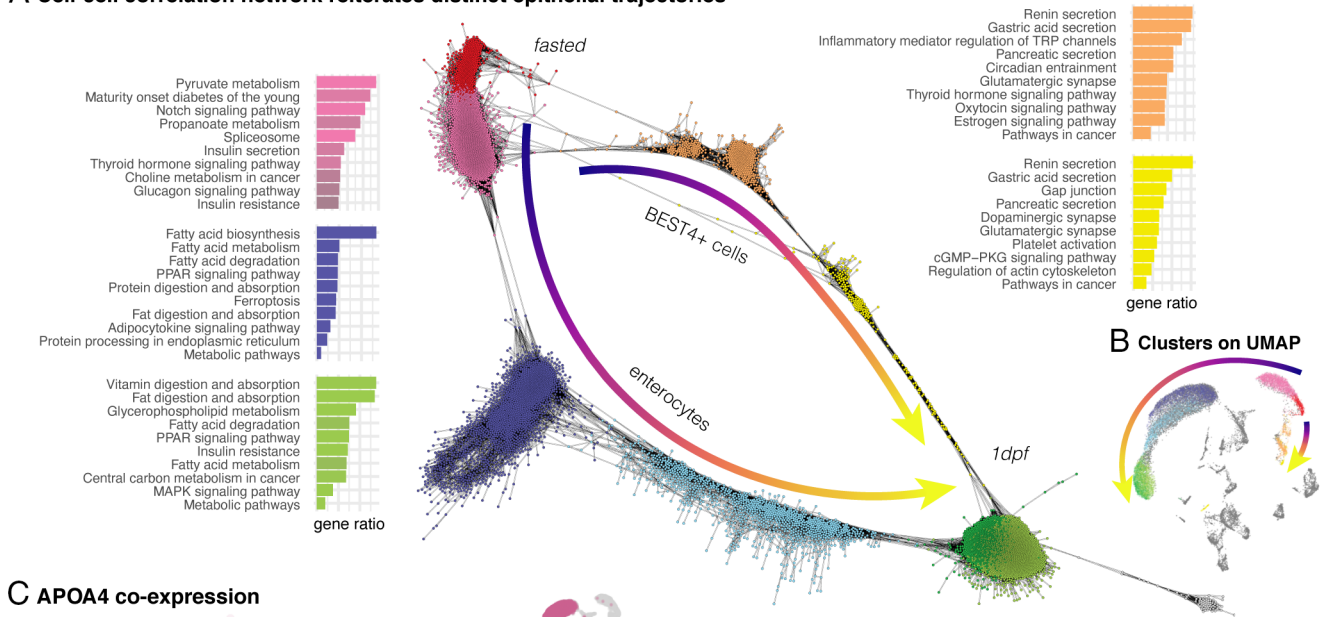
Fig. 3. Early intestinal restructuring driven by mesenchymal niche. (*A*) Signaling originating from mesenchymal cell clusters toward other clusters at 6 hrpf. Chord width indicates strength of signaling. LEC = lymphatic endothelial cells, EC = enterocytes, EEC = enteroendocrine cells, RBC = red blood cells, SM = smooth muscle, VEC = vascular endothelial cells. (*B*) Significant ligand–receptor pairs predicted to interact between indicated cell types. (*C*) Expression of PDGFRA from fasted to postfed tissue illustrating expansion of PDGFRA+ niche. (*D*) Top significantly differentially expressed genes between fibroblasts and stromal cells at 6 hrpf highlighting key expression of intestinal structure and regeneration regulators by stromal cells.

antibody staining that further indicates that they are most abundant in the mucosal epithelial layer (*SI Appendix*, Fig. S9). Evidence for their distinct trajectory during regeneration motivated us to explore intercellular and intracellular interactions associated with these cells. Other signaling interactions that we identified involving BEST4+ cells indicate that they are key modulators of inflammatory cell types (i.e., myeloid and endothelial cells) and exhibit high levels of intercellular cross talk compared to that observed in other absorptive epithelial cells (i.e., enterocytes; Figs. 4 and 5 and *SI Appendix*, Fig. S4). Through intercellular signaling interactions (Fig. 5*A*), BEST4+ cells express *DLL4* (Fig. 5 *B–D*), a NOTCH signaling ligand with well-established roles in coordinating cell–cell interactions and tissue patterning (39, 40) (Fig. 5 *B* and *D*). At the 6 hrpf and 12 hrpf timepoints, *DLL4* ligands expressed by BEST4+ cells are predicted to interact with *NOTCH1* receptors in endothelial and myeloid cell types (Fig. 5 *A* and *B*).
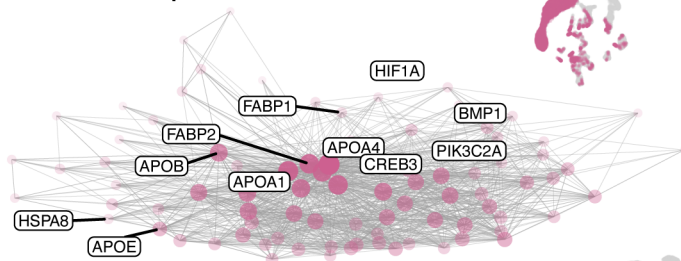
Our data and prior models of early signaling in snake intestinal regeneration (Fig. 1*A*) implicate the roles of early lipid metabolism

(via PPAR and APOA4 activation) and later inflammatory and stress responses (via the UPR/DDIT3; Fig. 1*A*) in promoting regenerative growth. Lipids are transported from the intestine by lacteals (intestinal villus lymphatic vessels) and *DLL4* expression activates their regenerative cycles separately from other regenerating intestinal tissue (41). Our results demonstrate upregulation of JAG1-, JAG2-, and DLL4-NOTCH1 signaling interactions between BEST4+ cells and lymphatic endothelial cells in postprandial python intestine (Fig. 5 *B* and *C*). These interactions coincide with extensive upregulation of other lipid-relevant metabolic and transport processes, including *DDIT3* (Fig. 5*C*), that accompany feeding and the early stages of the regenerative process. With respect to enterocytes, the postfeeding changes in gene regulatory network activity within BEST4+ cells are marked by the activity of two genes of note: a NOTCH coactivator (*ZMIZ1*) (42) and a transducer of mechanical signals (*SRF*) (43) (Fig. 5*C*). Evidence that BEST4+ cells, compared to enterocytes, also show greater numbers and higher strengths of interactions with other cell types between fasted and 6hpf reinforces the conclusion that
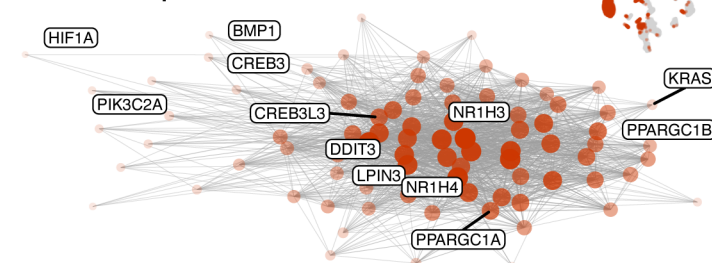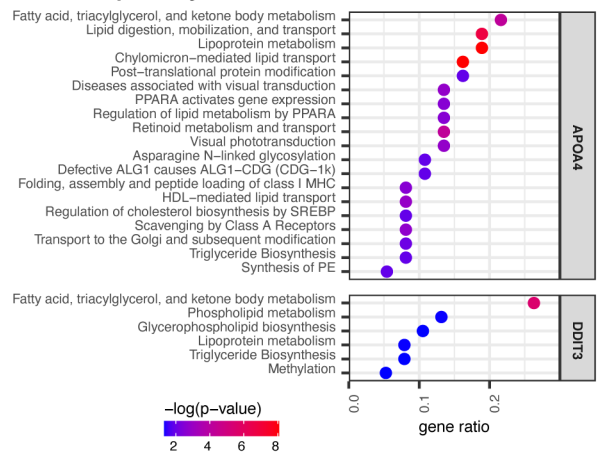
Fig. 4. Single-cell architecture of epithelial trajectories during regeneration. (*A*) Cell–cell correlation network of absorptive epithelial cells. *Inset* plots are KEGG pathway gene set enrichment ratios colored by cluster. (*B*) Correlation network-based epithelial cell clusters on the UMAP. (*C*) Coexpression networks of *APOA4* and (*D*) *DDIT3*, with *Inset* showing cells positive for network. (*E*) Significant functionally enriched pathways of *APOA4* and *DDIT3* networks.

BEST4+ cells play a role that is distinct from other absorptive cells during early phases of regeneration (*SI Appendix*, Fig. S4). These results collectively suggest that BEST4+ cells play a central role in regulation of regeneration via the primary ligand–receptor interaction DLL4-NOTCH1 which results in the dynamic reprogramming of other cells through the NOTCH signaling cascade.

Conserved Transcription Factor Regimes Reprogram Intestinal Metabolism. To test for evidence for the conservation of signaling mechanisms between pythons and humans, we compared broad TF regimes responsible for enterocyte activity changes throughout intestinal regeneration in pythons with those observed in a prior study of postgastric bypass metabolic reprogramming and restructuring in the human jejunum (44). We first used SCENIC (45) to determine all transcription factor (TF) regulons with high gene regulatory network activation and specificity among enterocyte cell clusters (Fig. 6A). Each phase of intestinal fasting

and regeneration displays distinct TF regimes in enterocytes. Fasted enterocytes have high specificity for regulons directed by KLF8, UBTF, KLF15, ARNTL2, and PDX1, which are involved in regulation of gluconeogenesis (46), intestinal morphogenesis (47), and insulin sensitivity (48–50). Throughout postfeeding regeneration, we identified progressive activation of nuclear receptors (NR1H4, NR1D2, PPARG, PPARGC1A) and regulators of stress response (NFE2L1, NFE2L2, ATF4, DDIT3, HIF1A) and intestinal cell identity (KLF6, MAFF) consistent with previous bulk RNAseq analyses (Fig. 1D). Using this set of TFs of interest, we next tested for activation of regulons derived from TF networks that were identified in prior work to be significantly expressed in postRYGB jejunum relative to normal human jejunum (44), a section of proximal intestine known for extensive structural and metabolic remodeling after gastric and duodenal bypass (11, 12), and identified several suites of responsive TFs shared between python and human jejunal regeneration with differential
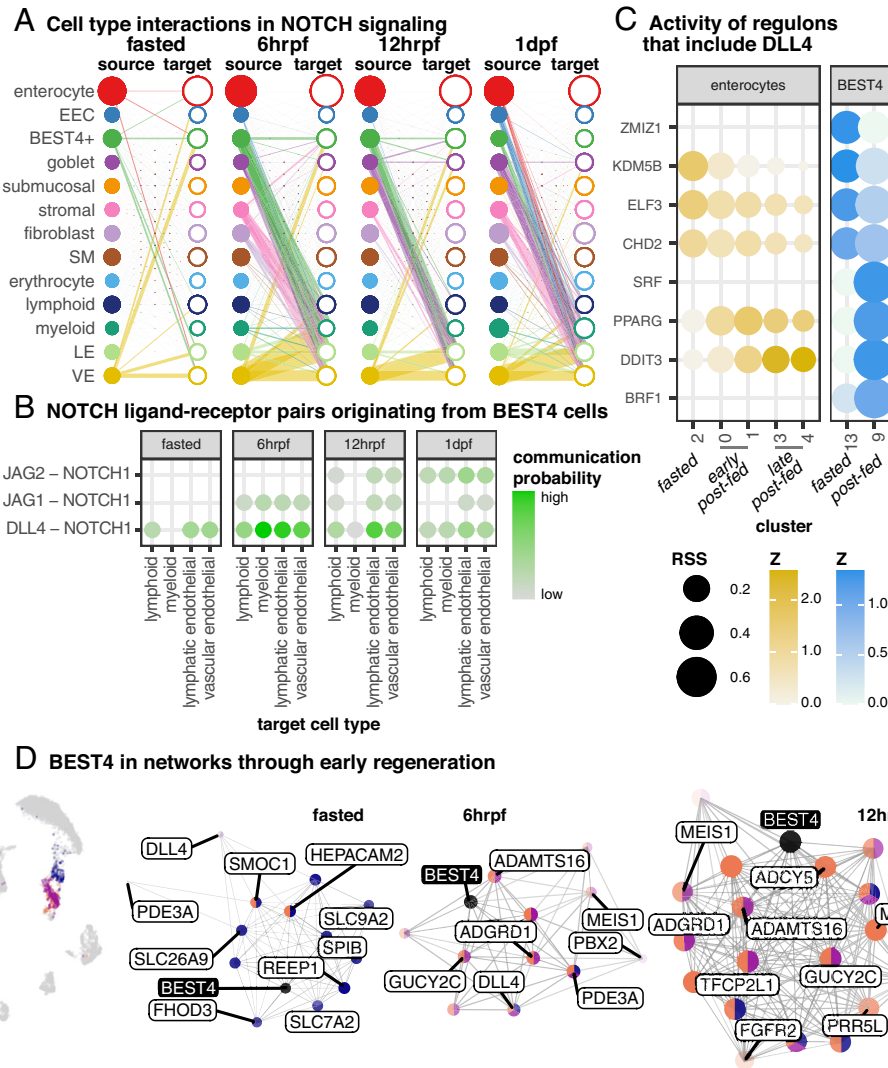
Fig. 5. BEST4 cells modulate lymphatic regeneration via DLL4. (*A*) Major source (ligand) and target (receptor) interactions of NOTCH signaling throughout regeneration. Line width indicates communication probability. Circle radii are scaled to number of cells. (*B*) Communication from BEST4 to endothelial and inflammatory cell types for NOTCH L-R pairs. (*C*) Regulon specificity and Z-score for regulons that include DLL4 with significant enrichment in enterocyte and BEST4 cell clusters. (*D*) Outgoing and incoming interaction strength for distinct cell types at time points pre- and postfeeding for the NOTCH signaling pathway. Dot size for each figure is proportional to the sum of the number of inferred interactions.
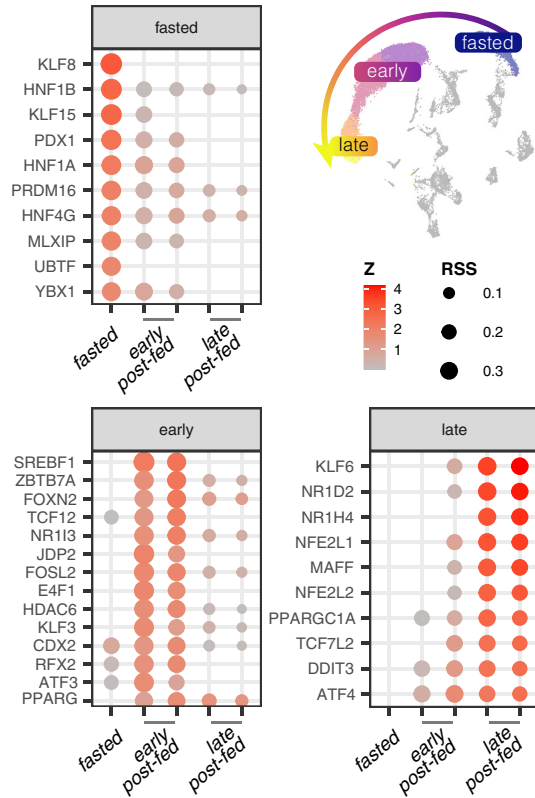
specificity across enterocyte clusters, including JUN, HIF1A, and PPARG (Fig. 6*B*). Two specific TFs—HNF1A and HNF1B—were inactivated in postprandial pythons, the opposite direction of their expression in the human jejunum after RYGB. HNF1A is a regulator of intestinal cell identity, and its loss amplifies mTOR signaling and crypt proliferation (51), and its downregulation in pythons might be critical to promoting extreme epithelial proliferation.

To further compare python intestinal regeneration to mammalian jejunal restructuring, we identified multiple genes that are specifically up- or downregulated in the jejunum after RYGB in mice and humans (52). We found broad similarity with the expression of upregulated genes in python proximal small intestine (Fig. 6*C*), except for a subset of glutamate metabolism genes that are downregulated in pythons (Fig. 6*C*). RYGB reprograms lipid handling among rat enterocytes by downregulation of specific genes during fasting, including *APOA4* (53); all of these that could be identified in the python snRNAseq data are downregulated when fasting and upregulated postfeeding (Fig. 6*B*). These findings reveal broad similarities between python postfeeding regenerative

responses and RYGB in mammals that suggest a common and conserved regulatory program across vertebrates.
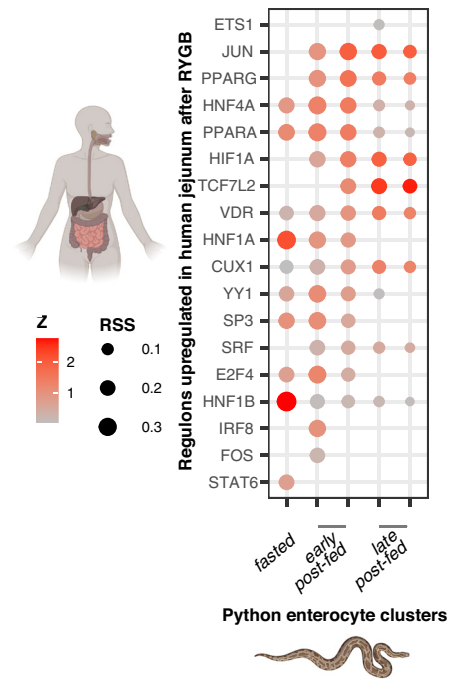
Prior work has proposed that Wnt signaling may also play key roles in python intestinal regeneration (8, 21). To explore this further, we examined patterns of expression for gene associated with Wnt signaling across cell types and timepoints (*SI Appendix*, Fig. S10). We find that *LRP5* and *LRP6*, homologous coreceptors of Wnt ligands (54), are expressed in the highest fraction of cells in late postfeeding enterocytes and mesenchymal cells. LRP6 showed the highest expression levels at 1 dfp, and LRP5 showed the highest expression in fasted cells (*SI Appendix*, Fig. S10). Additionally, we observed expression of a major downstream transcription factor in the Wnt pathway, TCF7L2, across multiple time points, at its highest levels (average per cell) at 1 dpf, and expressed in the highest fraction of late postprandial enterocytes and mesenchymal cells (*SI Appendix*, Fig. S10). These results reinforce the evidence for a role of Wnt signaling during python intestinal regeneration that appears most active in late postfeeding stages (1 dpf) and which appears associated with early activity of LRP5 and a later increase of LRP6 activity around 1 dpf.
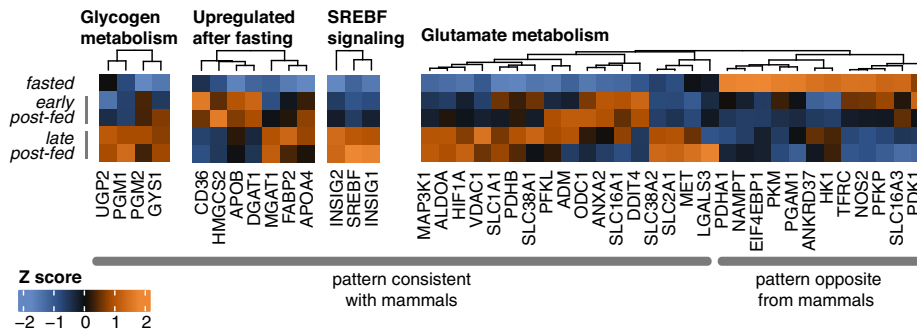
Fig. 6. Metabolic reprogramming in postprandial python enterocytes resembles architecture of postgastric bypass intestinal adaptations. (*A*) Top regulons from SCENIC activated in enterocyte clusters, separated by timing of peak activation during python regeneration. Z scores less than or equal to zero are dropped. *Inset* UMAP shows clusters. (*B*) Python activation of regulon set that is upregulated after RYGB to support human intestinal remodeling. The set of genes expressed post RYGB in humans was obtained from a prior study (44). (*C*) Expression throughout regeneration of genes annotated in python that are upregulated in jejunum of mice or humans after RYGB. Gray lines indicate genes that are expressed either in a consistent or opposite pattern in pythons relative to mammals. Genes differentially expressed postmammalian RYGB were obtained from a prior study (52).

Discussion

Diverse models of vertebrate regeneration provide valuable opportunities to identify potentially conserved mechanisms that expand our understanding of vertebrate intestinal physiology and regenerative capacity (55–57). Here, we identify molecular and cellular processes that coordinate extreme intestinal regeneration in pythons, and we provide unique evidence for conserved cell-type-specific roles that mediate vertebrate intestinal regeneration and differentiation. Our findings support the existence of conserved intestinal regenerative capacity that may be common to most vertebrates, including humans, involving distinct regulation by BEST4+ and

mesenchymal cells. These regenerative programs recapitulate programs co-opted from early development and wound healing pathways conserved across vertebrates. These findings raise additional questions about the role of intestinal crypt populations in vertebrates and whether they are indeed the only source of stem cells for renewal and differentiation, as well as the degree to which other cell populations (e.g., BEST4+ enterocytes and mesenchymal cells) also contribute to vertebrate differentiation and regenerative capacity. Our findings in pythons also provide a different perspective on noncanonical functional roles of CHOP/DDIT3 signaling.

The lack of crypts and cyclic villus atrophy unique to python intestinal regeneration provides distinct insight into the degree to which

nonenterocyte cell types coordinate regenerative programming. Consistent with emerging evidence for the roles of mesenchymal cells in mammalian intestinal differentiation (58), our single-cell resolution implicates key roles for mesenchymal cells, such as fibroblasts and stromal cells, in orchestrating major tissue differentiation via cell–cell communication to coordinate growth, axon guidance, inflammation, and tissue patterning pathways. Our results illustrate that mesenchymal cells operate distinct signaling programs entirely distinct from the epithelium and engage in the greatest number of intercellular interactions with other mesenchymal cell types and with the endothelium. The ECM and adhesion dynamics implicated by intercellular signaling patterns of mesenchymal cells during python intestinal regeneration parallel similar dynamics observed early in embryonic mouse villus development. In the mouse, PDGFRA^high stromal cells are critical for initiating villus extension (34). The high expression of nonfibrillar collagen genes in python stromal cells observed align with PDGFRA^high embryonic mesenchyme in mice (34). The python mesenchyme also expresses high *NRG1*, an activator of stem cell proliferation and tissue regeneration after damage (28). Collectively, our results indicate that early python intestinal regeneration involves the joint activation of pseudoembryonic restructuring and canonical wound healing mechanisms in the intestinal mesenchymal niche to promote villus growth. This conclusion, together with parallel evidence from mammalian systems (34, 58), motivates future work to investigate the roles and capabilities of the mesenchyme to direct regenerative growth in vertebrate systems.

Our single-cell data also provide evidence for distinct roles of BEST4+ cells in coordinating intestinal regeneration in the python, and potentially humans, that has otherwise been obscured by work in mammalian models that lack these cells. While BEST4+ cells occur throughout the small intestine and colon in humans, they are found only in the posterior intestinal tract of zebrafish (59) and are absent from mice (60). Due to their recent discovery and relatively low frequency, BEST4+ cells in the GI tract have received limited characterization. They have been hypothesized to function in pH homeostasis, inflammation, and proliferation, and their functional roles appear conserved across model systems in which they have been observed (31, 59, 61, 62). Our single cell and histological data identify a relatively large population of BEST4+ cells from the proximal small intestine that show remarkably distinct expression programs from other epithelial cells throughout regeneration. Postfeeding, python intestinal BEST4+ cells transcriptional programs resemble conserved profiles identified from human and zebrafish BEST4+ cells, including expression of *OTOP2*, *SPIB*, *GUC2YC*, and NOTCH pathway genes.

Our python single-cell data illustrate how BEST4+ cells act as a key hub of integration for multiple diverse signals, including those from hormones and nerve synapses, and communicate with other cell types while also expressing a portion of the same metabolic and stress pathways as enterocytes. These results also indicate that in postprandial python intestine, BEST4+ cells coordinate cell–cell signaling interactions with lymphatic endothelial cells to upregulate DLL4-NOTCH1 signaling. Lipids are transported from the intestine by lacteals (intestinal villus lymphatic vessels) and DLL4 expression activates their regenerative cycles separately from other regenerating intestinal tissue (41). The significance of NOTCH signaling in gastrointestinal regeneration is highlighted by observations from different biological contexts. NOTCH pathway signaling has been implicated for its role in fostering gastric stem cell proliferation and the onset of gastric tumors (63). Other work has suggested that a hierarchical relationship between NOTCH and mTOR exists, whereby NOTCH can activate mTOR (64, 65). This

suggests that in pythons, BEST4+ cells are a central regulator of early regeneration via the NOTCH and potentially mTOR signaling cascades, and they specifically regulate lacteal formation and lipid metabolism to promote regeneration.

Among epithelial cell types in the python small intestine, only goblet cells show evidence of an expansion in their number from fasted to 1 dpf, based on relative fractions of cell types resolved by snRNAseq (*SI Appendix*, Fig. S2). This relative increase in goblet cells appears to coincide with an increase in their role in intercellular ligand–receptor signaling at 6 hrpf (*SI Appendix*, Fig. S4E). This signaling involves their reception of signals related to cell adhesion and patterning from submucosal, stromal, fibroblast and smooth muscle cells (*SI Appendix*, Fig. S4 *B* and *D*). This postfeeding increase in goblet cell signaling is also associated with an increase of NOTCH signaling from goblet cells at 12 hrpf (Fig. 5D). This suggests that, despite making up a small fraction of all intestinal cells (similar to BEST4+), goblet cells also play critical postfeeding roles in mucus secretion and signaling during regeneration.

Our findings in pythons have broad relevance for understanding the roles of lipid metabolism, insulin, and stress response in modulating both intestinal regeneration and metabolic and cellular reprogramming in vertebrates. Our results expand upon prior suggestions for a role of Wnt signaling in python intestinal regenerative reprogramming (8, 21) and identify Wnt activity primarily driven by the high-level transcription factor TCF7L2, which is associated with especially high expression in late postfeeding enterocytes and mesenchymal cells. Wnt ligands LRP5/6 have established functions in glucose and cholesterol metabolism and homeostasis (66), and the contrasting temporal patterns of expression during python regeneration suggest distinct roles for these ligands under fasting vs. postfeeding regenerative states in the python intestine. Although *LRP6* expression is not typically associated with the small intestine, the high expression of LRP6 and TCF7L2 at 1 dpf likely contributes to transformations in glucose metabolism, mTOR signaling, and insulin responsiveness we observe in the late postfeeding regeneration response (67, 68). These findings reinforce other previous conclusions (8, 21–23) that rapid switches in growth and stress pathway signaling coordinate snake intestinal regeneration and provide insight into the critical role for lipid metabolism-focused signaling and the closely linked activation of *DDIT3*. The strongest early postfeeding response we observed was the upregulation of lipid metabolism in enterocytes, driven by PPAR and apolipoprotein signaling, and the subsequent activation of *DDIT3*. Our results suggest that this early response plays a critical role in directing major metabolic and proliferative regulatory genes in a manner typically associated with pathological and not physiological contexts (69), highlighting perspectives on the potential roles of *DDIT3* signaling in regeneration. Specifically, *DDIT3* is traditionally viewed as the pro-apoptotic branch of the UPR (70), with some evidence that it plays a role in lipid metabolism through activation by its upstream effector, PERK (71). In the python regenerative intestinal model, it appears to promote rapid metabolic switches and cell survival under extreme stress, analogous to that observed in tumors in response to glutamine starvation and metabolic stress (69). This evidence for the functional roles of *DDIT3* signaling that conflict with canonical views of its activity would be a priority to investigate in follow-up studies.

Expression of *APOA4*, a key component of postprandial enterocyte responses in our data, occurs at the center of a massive lipid regulatory pathway connected to nuclear receptors previously identified as playing critical roles in snake organ regeneration (e.g., PPAR, LXR/RXR, and FXR) (21, 22, 72). Consistent

with a conserved role in early-phase regenerative intestinal reprogramming, *APOA4* has also been implicated in postgastric bypass metabolic remodeling in mammalian jejunum (52). *APOA4* has broad antioxidant and anti-inflammatory functionality and influence over glucose homeostasis and insulin secretion (73). Our findings suggest that *RBP2* and *FABP2* coordinate the activity of *APOA4* underlying the early postprandial lipid response. Interestingly, while these proteins are thought to be critical for small intestinal epithelial growth and metabolism (74, 75), they are not expressed in fasted python small intestine enterocytes (*SI Appendix*, Fig. S8). This suggests that fasted python enterocytes undergo fundamental changes to their physiology (distinct from typical enterocyte function) that is restored and regulated by *APOA4* in the early postfeeding response phase. These findings collectively suggest a key role for lipid metabolism-focused signaling and the closely linked activation of *DDIT3*, with connections to widely conserved signaling regimes that involve nuclear receptors (*PPARA*, *PPARG*, *NR1H3*, and *NR1H4*), PI3K (*PIK3C2A*), *CREB3* metabolic pathways, and stress responses (*HIF1A*, *HSPA8*, and *CHOP/DDIT3*).

Taken together, python postprandial and human RYGB data reinforce emerging evidence for the intestine as a secondary hub of metabolic regulation that interacts with both insulin sensitivity and blood glucose (12). Our findings in pythons uncover transformative metabolic reprogramming in enterocytes via multiple conserved lipid, glucose, and stress response regulatory pathways that, in mammals, broadly regulate glucose tolerance and insulin responsiveness and are only achieved after extensive surgical intervention (11, 12). The mechanisms that manage cyclic metabolic stress and nutrient overload in python intestine provide insight that may finally explain the otherwise poorly known mechanisms leading to RYGB. Our findings suggest that nutrient overload may trigger highly conserved regenerative and redifferentiation mechanisms that explains both the human RYGB redifferentiation as well as its profound effectiveness in curing type II diabetes. Indeed, during regeneration, python enterocytes also express key markers and transcription factor regulons that recapitulate mammalian intestinal and metabolic reprogramming after RYGB. Python intestinal regeneration shares many key features with human RYGB, suggesting that these regenerative mechanisms may be highly conserved across vertebrates.

Materials and Methods

Animal Care and Feeding Experiments. All animal care and experimentation were conducted at the University of Alabama under an approved IACUC protocol in AAALAC-accredited facilities (14-06-00075). Burmese pythons were obtained captive-bred and maintained in a standard rack housing system. They were fasted to a postabsorptive Phase III fasted state prior to experimentation, then fed meals sized to 25% of their body mass. Snakes were randomly assigned time point–based sample groups of fasted (n = 5), 6 hrpf (n = 3), 12 hrpf (n = 4), 1 dpf (n = 3), 3 dpf (n = 4), and 6 dpf (n = 4; total n = 23) and were euthanized via severing of the spinal cord at the base of the skull, according to the approved procedure by the University of Alabama Institutional Animal Care and Use Committee (IACUC). Small intestine tissue was immediately dissected and snap-frozen for downstream use.

RNAseq and Gene Expression Analysis. We used a standard Trizol Reagent (Invitrogen) protocol to extract total RNA from approximately 50 mg of snap-frozen tissue. RNA was sent to Novogene Co (Davis, CA), who constructed libraries for mRNA sequencing with the TruSeq Stranded mRNA kit (Illumina). Libraries were then pooled and sequenced on an Illumina NovaSeq to produce 150 bp paired-end reads. Reads were de-multiplexed prior to data receipt. Raw reads were quality filtered with Trimmomatic 0.36 (76) then mapped and quantified against the Burmese python reference genome (27) with STAR 2.7.10a (77).

Counts were normalized and pairwise tests between consecutive time points (e.g., fasted vs. 6 hrpf) were conducted with DESeq2 1.36.0 (78) in R. Differentially expressed genes were hierarchically clustered and visualized by pheatmap 1.0.12 (79). We imported these results to Ingenuity Pathway Analysis (IPA) (Qiagen Inc.) using the core analysis function to estimate URM activation and construct mechanistic networks.

Single-Nucleus RNAseq and Analysis. We sent 200 mg of snap-frozen small intestine each from snakes from fasted, 6 hrpf, 12 hrpf, and 1 dpf (n = 1 each; total n = 4) to SingulOmics Corporation (Bronx, NY). There, nuclei were isolated and partitioned, and libraries were prepared for single nucleus RNAseq via the 10× Genomics Chromium platform. The 1 dpf samples was sequenced in advance to validate the method in snake intestinal tissue, and subsequently the fasted, 6 hrpf, and 12 hrpf were multiplexed and sequenced together. We mapped the de-multiplexed reads to the Burmese python reference genome with 10× Genomics Cell Ranger 6.1.1. Counts and metadata were imported into Seurat 4.2.0 (80) for quality filtered, normalization and scaling, and clustering following standard protocol. Cells were clustered using the top 16 principal components, as determined from an elbow plot, and visualized with Universal Manifold Approximation (UMAP). Cluster cell type identity were determined by marker gene expression: enterocytes (EPCAM, APOB), BEST4+ cells (BEST4, OTOP2), goblet cells (AGR2, SPDEF, MUC2), enteroendocrine cells (CHGA, CCK, GCG), fibroblasts (VIM, FAP), smooth muscle (DES, MYH11), mesenchymal cells (PDGFRA, OGN, COL3A1), stromal cells (PDGFRA, BMP5), lymphoid lineage cells (PTPRC), myeloid lineage cells (CSF1R), erythrocytes (ANK1, HEMGN), vascular endothelium (FLT1, PECAM1), and lymphatic endothelium (LYVE1, PECAM1). Cell-cell networks were constructed with Graphia (81) from the Pearson correlations of the top 50 PCs and the Louvain method for clustering. These were analyzed for differential expression with Seurat and functional enrichment with WebGestalt (82). We calculated intercellular networks, identified their presence in cells, and performed functional enrich with fcoex 1.10.0 (83) in R. Intercellular signaling was measured and analyzed with cellchat 1.5.0 (84). and transcription factor regulons were inferred and analyzed with the SCENIC 1.3.1 (45, 85) pipeline. Gene lists for genes expressed post-RYGB in humans (44) and for differentially expressed mammalian (human and mice) genes pre- and post-RYGB (52) (NCBI GEO: GSE112823) were obtained from prior studies.

Cryosectioning, Immunohistochemistry, and Microscopy. Sections of python fasted and 1 dpf small intestine tissue that had been everted and flash-frozen were sectioned on a cryostat and embedded in 50/50 OCT/Tissue Freezing Medium solution. Sections were cut serially and either stained with H&E or with BEST4 polyclonal antibody (ThermoFisher Scientific [catalog# BS-11043R], Bioss, 1:400) and counterstained with hematoxylin. BEST4 stained tissues were washed three times in TBS and blocked for 1 h using 10% normal goat serum in TBS. BEST4 antibody in TBS + 10% normal goat serum was then added, and the sections were incubated overnight at 4 °C in a humidified chamber. After incubation, sections were washed three times in TBS and incubated with a secondary antibody for 1 h. Sections were then washed three times in TBS and incubated for 30 min with ABC solution. We then washed the sections three times in TBS and added DAB solution (Vector, SK-4100) for 5 min and quenched the reaction in ddH$_2$O. All samples were washed three times in TBS and mounted in 50% glycerol. Samples were then imaged using a NanoZoomer S60 at the UT Southwestern Whole Brain Microscopy Facility.

Data, Materials, and Software Availability. Scripts used for data analysis are available on GitHub at https://github.com/akwestfall/PythonSingleNucleus (86). Raw single-nucleus and bulk RNAseq have been deposited to the NCBI SRA under the BioProject accession PRJNA1080230 (87).

Author affiliations: ªDepartment of Biology, University of Texas at Arlington, Arlington, TX 76019; ᵇChildren's Medical Center Research Institute, University of Texas Southwestern Medical Center, Dallas, TX 75235; ᶜDepartment of Biological Sciences, University of Alabama, Tuscaloosa, AL 35401; and ᵈDepartment of Chemistry and Biochemistry, University of Texas at Arlington, Arlington, TX 76019

1. J. M. Williams et al., Epithelial cell shedding and barrier function: A matter of life and death at the small intestinal villus tip. Vet. Pathol. 52, 445–455 (2015).
2. R. M. Houtekamer, M. C. van der Net, M. M. Maurice, M. Gloerich, Mechanical forces directing intestinal form and function. Curr. Biol. 32, R791–R805 (2022).
3. L. G. van der Flier, H. Clevers, Stem cells, self-renewal, and differentiation in the intestinal epithelium. Ann. Rev. Physiol. 71, 241–260 (2009).
4. J.-H. Lignot, C. Helmstetter, S. M. Secor, Postprandial morphological response of the intestinal epithelium of the Burmese python (Python molurus). Comp. Biochem. Physiol. A: Mol. Integr. Physiol. 141, 280–291 (2005).
5. S. M. Secor, J. Diamond, Determinants of the postfeeding metabolic response of Burmese pythons, Python molurus. Physiol. Zool. 70, 202–212 (1997).
6. S. M. Secor, J. Diamond, Adaptive responses to feeding in Burmese pythons: Pay before pumping. J. Exp. Biol. 198, 1313–1325 (1995).
7. J. M. Starck, K. Beese, Structural flexibility of the intestine of Burmese python in response to feeding. J. Exp. Biol. 204, 325–335 (2001).
8. A. L. Andrew et al., Rapid changes in gene expression direct rapid shifts in intestinal form and function in the Burmese python after feeding. Physiol. Genomics 47, 147–157 (2015).
9. S. M. Secor, J. M. Diamond, Evolution of regulatory responses to feeding in snakes. Physiol. Biochem. Zool. 73, 123–141 (2000).
10. S. M. Secor, H. V. Carey, Integrative physiology of fasting. Compr. Physiol. 6, 773–825 (2016).
11. J. P. Thaler, D. E. Cummings, Hormonal and metabolic mechanisms of diabetes remission after gastrointestinal surgery. Endocrinology 150, 2518–2525 (2009).
12. P. Sala et al., Type 2 diabetes remission after Roux-en-Y Gastric bypass: Evidence for increased expression of jejunal genes encoding regenerating pancreatic islet-derived proteins as a potential mechanism. Obes. Surg. 27, 1123–1127 (2017).
13. V. Kamvissi-Lorenz, M. Raffaelli, S. Bornstein, G. Mingrone, Role of the gut on glucose homeostasis: Lesson learned from metabolic surgery. Curr. Atheroscler. Rep. 19, 9 (2017).
14. L. Elli et al., Small bowel villous atrophy: Celiac disease and beyond. Expert Rev. Gastroenterol. Hepatol. 11, 125–138 (2017).
15. D. Dahlgren, M. Sjöblom, P. M. Hellström, H. Lennernäs, Chemotherapeutics-induced intestinal mucositis: Pathophysiology and potential treatment strategies. Front. Pharmacol. 12, 681417 (2021).
16. B. J. Sheahan et al., Epithelial regeneration after doxorubicin arises primarily from early progeny of active intestinal stem cells. Cell. Mol. Gastroenterol. 12, 119–140 (2021).
17. X. Zhu et al., Quercetin mitigates radiation-induced intestinal injury and promotes intestinal regeneration via Nrf2-mediated antioxidant pathway1. Radiat. Res. 199, 252–262 (2023).
18. S. M. Secor, D. Fehsenfeld, J. Diamond, T. E. Adrian, Responses of python gastrointestinal regulatory peptides to feeding. Proc. Natl. Acad. Sci. U.S.A. 98, 13637–13642 (2001).
19. M. Otaka, M. Odashima, S. Watanabe, Role of heat shock proteins (molecular chaperones) in intestinal mucosal protection. Biochem. Biophys. Res. Commun. 348, 1–5 (2006).
20. M. A. McGuckin, R. D. Eri, I. Das, R. Lourie, T. H. Florin, ER stress and the unfolded protein response in intestinal inflammation. Am. J. Physiol. Gastrointest. Liver Physiol. 298, G820–G832 (2010).
21. A. L. Andrew et al., Growth and stress response mechanisms underlying post-feeding regenerative organ growth in the Burmese python. BMC Genomics 18, 338 (2017).
22. A. K. Westfall et al., Identification of an integrated stress and growth response signaling switch that directs vertebrate intestinal regeneration. BMC Genomics 23, 6 (2022).
23. B. W. Perry et al., Multi-species comparisons of snakes identify coordinated signalling networks underlying post-feeding intestinal regeneration. Proc. R. Soc. B Biol. Sci. 286, 20190910 (2019).
24. A. Ayyaz et al., Single-cell transcriptomes of the regenerating intestine reveal a revival stem cell. Nature 569, 121–125 (2019).
25. W. D. Rees, R. Tandun, E. Yau, N. C. Zachos, T. S. Steiner, Regenerative intestinal stem cells induced by acute and chronic injury: The saving grace of the epithelium? Front. Cell Dev. Biol. 8, 583919 (2020).
26. A. L. Hauck et al., Twists and turns in the development and maintenance of the mammalian small intestine epithelium. Birth Defects Res. C: Embryo Today 75, 58–71 (2005).
27. T. A. Castoe et al., Sequencing the genome of the Burmese python (Python molurus bivittatus) as a model for studying extreme adaptations in snakes. Genome Biol. 12, 1–8 (2011).
28. T. Jardé et al., Mesenchymal niche-derived neuregulin-1 drives intestinal stem cell proliferation and regeneration of damaged epithelium. Cell Stem Cell 27, 646–662.e7 (2020).
29. I. V. Pinchuk, R. C. Mifflin, J. I. Saada, D. W. Powell, Intestinal mesenchymal cells. Curr. Gastroenterol. Rep. 12, 310–318 (2010).
30. J. Beumer et al., High-resolution mRNA and secretome atlas of human enteroendocrine cells. Cell 181, 1291–1306.e19 (2020).
31. R. Elmentaite et al., Cells of the human intestinal tract mapped across space and time. Nature 597, 250–255 (2021).
32. G. Greicius, D. M. Virshup, Stromal control of intestinal development and the stem cell niche. Differentiation 108, 8–16 (2019).
33. K. D. Walton, D. Mishkind, M. R. Riddle, C. J. Tabin, D. L. Gumucio, Blueprint for an intestinal villus: Species-specific assembly required. WIREs Dev. Biol. 7, e317 (2018).
34. T. R. Huycke et al., Patterning and folding of intestinal villi by active mesenchymal dewetting. bioRxiv [Preprint] (2023), https://doi.org/10.1101/2023.06.25.546328 (Accessed 12 March 2024).
35. T. T. Lemmetyinen et al., Fibroblast-derived EGF ligand neuregulin 1 induces fetal-like reprogramming of the intestinal epithelium without supporting tumorigenic growth. Dis. Model Mech. 16, dmm049692 (2023).
36. J. H. Won, J. S. Choi, J.-I. Jun, CCN1 interacts with integrins to regulate intestinal stem cell proliferation and differentiation. Nat. Commun. 13, 3117 (2022).
37. J. H. van Es et al., Dll1+ secretory progenitor cells revert to stem cells upon crypt damage. Nat. Cell Biol. 14, 1099–1104 (2012).
38. J. Beumer et al., BMP gradient along the intestinal villus axis controls zonated enterocyte and goblet cell states. Cell Rep. 38, 110438 (2022).
39. J. R. Shutter et al., Dll4, a novel Notch ligand expressed in arterial endothelium. Genes Dev. 14, 1313–1318 (2000).
40. M. Hellström et al., Dll4 signalling through Notch1 regulates formation of tip cells during angiogenesis. Nature 569, 776–780 (2007).
41. J. Bernier-Latmani et al., DLL4 promotes continuous adult intestinal lacteal regeneration and dietary fat transport. J. Clin. Invest. 125, 4572–4586 (2015).
42. N. Pinnell et al., The PIAS-like coactivator Zmiz1 is a direct and selective cofactor of Notch1 in T cell development and leukemia. Immunity 43, 870–883 (2015).
43. J. M. Miano, X. Long, K. Fujiwara, Serum response factor: Master regulator of the actin cytoskeleton and contractile apparatus. Am. J. Physiol. Cell Physiol. 292, C70–C81 (2007).
44. M. A. Stefater-Richards et al., Gut adaptation after gastric bypass in humans reveals metabolically significant shift in fuel metabolism. Obesity 31, 49–61 (2023).
45. S. Aibar et al., SCENIC: Single-cell regulatory network inference and clustering. Nat. Methods 14, 1083–1086 (2017).
46. S. Gray et al., Regulation of gluconeogenesis by Krüppel-like factor 15. Cell Metab. 5, 305–312 (2007).
47. C. Chen, E. Sibley, Expression profiling identifies novel gene targets and functions for Pdx1 in the duodenum of mature mice. Am. J. Physiol. Gastrointest. Liver Physiol. 302, G407–G419 (2012).
48. D. Y. Jung et al., KLF15 is a molecular link between endoplasmic reticulum stress and insulin resistance. PLoS One 8, e77851 (2013).
49. M.-S. Hung, P. Avner, U. C. Rogner, Identification of the transcription factor ARNTL2 as a candidate gene for the type 1 diabetes locus Idd6. Hum. Mol. Genet. 15, 2732–2742 (2006).
50. C.-X. He, N. Prevot, C. Boitard, P. Avner, U. C. Rogner, Inhibition of type 1 diabetes by upregulation of the circadian rhythm-related aryl hydrocarbon receptor nuclear translocator-like 2. Immunogenetics 62, 585–592 (2010).
51. C. R. Lussier et al., Loss of hepatocyte-nuclear-factor-1α impacts on adult mouse intestinal epithelial cell growth and cell lineages differentiation. PLoS One 5, e12378 (2010).
52. D. Ben-Zvi et al., Time-dependent molecular responses differ between gastric bypass and dieting but are conserved across species. Cell Metab. 28, 310–323 (2018).
53. S. Kaufman et al., Roux-en-Y gastric bypass surgery reprograms enterocyte triglyceride metabolism and postprandial secretion in rats. Mol. Metab. 23, 51–59 (2019).
54. Q. Ren, J. Chen, Y. Liu, LRP5 and LRP6 in Wnt signaling: Similarity and divergence. Front. Cell Dev. Biol. 9, 670960 (2021).
55. E. D. Hutchins et al., Transcriptomic analysis of tail regeneration in the lizard Anolis carolinensis reveals activation of conserved vertebrate developmental and repair mechanisms. PLoS One 9, e105004 (2014).
56. A. Joven, A. Elewa, A. Simon, Model systems for regeneration: Salamanders. Development 146, dev167700 (2019).
57. M. Gemberling, T. J. Bailey, D. R. Hyde, K. D. Poss, The zebrafish as a model for complex tissue regeneration. Trends Genet. 29, 611–620 (2013).
58. H. M. Kolev, K. H. Kaestner, Mammalian intestinal development and differentiation–The state of the Art. Cell. Mol. Gastroenterol. Hepatol. 16, 809–821 (2023).
59. R. J. Willms, L. O. Jones, J. C. Hocking, E. Foley, A cell atlas of microbe-responsive processes in the zebrafish intestine. Cell Rep. 38, 110311 (2022).
60. H. Fazilaty et al., Tracing colonic embryonic transcriptional profiles and their reactivation upon intestinal damage. Cell Rep. 36, 109484 (2021).
61. G. A. Busslinger et al., Human gastrointestinal epithelia of the esophagus, stomach, and duodenum resolved at single-cell resolution. Cell Rep. 34, 108819 (2021).
62. J. Burclaff et al., A proximal-to-distal survey of healthy adult human small intestine and colon epithelium by single-cell transcriptomics. Cell. Mol. Gastroenterol. Hepatol. 13, 1554–1589 (2022).
63. E. S. Hibdon et al., Notch and mTOR signaling pathways promote human gastric cancer cell proliferation. Neoplasia 21, 702–712 (2019).
64. S. M. Chan, A. P. Weng, R. Tibshirani, J. C. Aster, P. J. Utz, Notch signals positively regulate activity of the mTOR pathway in T-cell acute lymphoblastic leukemia. Blood 110, 278–286 (2007).
65. T. Palomero et al., Mutational loss of PTEN induces resistance to NOTCH1 inhibition in T-cell leukemia. Nat. Med. 13, 1203–1210 (2007).
66. D. M. Joiner, J. Ke, Z. Zhong, H. E. Xu, B. O. Williams, LRP5 and LRP6 in development and disease. Trends Endocrinol. Metab. 24, 31–39 (2013).
67. R. Singh et al., LRP6 enhances glucose metabolism by promoting TCF7L2-dependent insulin receptor expression and IGF receptor stabilization in humans. Cell Metab. 17, 197–209 (2013).
68. W. Ip, Y. A. Chiang, T. Jin, The involvement of the wnt signaling pathway and TCF7L2 in diabetes mellitus: The current understanding, dispute, and perspective. Cell Biosci. 2, 28 (2012).
69. M. Li et al., DDIT3 directs a dual mechanism to balance glycolysis and oxidative phosphorylation during glutamine deprivation. Adv. Sci. (Weinh) 8, e2003732 (2021).
70. Y. Li, Y. Guo, J. Tang, J. Jiang, Z. Chen, New insights into the roles of CHOP-induced apoptosis in ER stress. Acta Biochim. Biophys. Sin. (Shanghai) 47, 146–147 (2015).
71. M. Moncan et al., Regulation of lipid metabolism by the unfolded protein response. J. Cell. Mol. Med. 25, 1359–1370 (2021).
72. J. A. Magida et al., Burmese pythons exhibit a transient adaptation to nutrient overload that prevents liver damage. J. Gen. Physiol. 154, e202113008 (2022).
73. F. Wang et al., Apolipoprotein A-IV: A protein intimately involved in metabolism. J. Lipid Res. 56, 1403–1418 (2015).
74. P. Besnard, I. Niot, H. Poirier, L. Clément, A. Bernard, "New insights into the fatty acid-binding protein (FABP) family in the small intestine" in Cellular Lipid Binding Proteins, J. F. C. Glatz, Ed. (Springer US, 2002), pp. 139–147.
75. R. M. Calderon et al., Intestinal enteroendocrine cell signaling: Retinol-binding protein 2 and retinoid actions. Endocrinology 163, bqac064 (2022).
76. A. M. Bolger, M. Lohse, B. Usadel, Trimmomatic: A flexible trimmer for Illumina sequence data. Bioinformatics 30, 2114–2120 (2014).
77. A. Dobin et al., STAR: Ultrafast universal RNA-seq aligner. Bioinformatics 29, 15–21 (2013).
78. M. I. Love, W. Huber, S. Anders, Moderated estimation of fold change and dispersion for RNA-seq data with DESeq2. Genome Biol. 15, 1–21 (2014).
79. R. Kolde, M. R. Kolde, Package 'pheatmap'. R Package 1, 790 (2015).
80. Y. Hao et al., Integrated analysis of multimodal single-cell data. Cell 184, 3573–3587.e29 (2021).
81. T. C. Freeman et al., Graphia: A platform for the graph-based visualisation and analysis of high dimensional data. PLoS Comput. Biol. 18, e1010310 (2022).
82. Y. Liao, J. Wang, E. J. Jaehnig, Z. Shi, B. Zhang, WebGestalt 2019: Gene set analysis toolkit with revamped UIs and APIs. Nucleic Acids Res. 47, W199–W205 (2019).
83. T. Lubiana, H. Nakaya, Using coexpression to explore cell-type diversity with the fcoex package. bioRxiv [Preprint] (2021). https://doi.org/10.1101/2021.12.07.471503v1 (Accessed 14 February 2024).
84. S. Jin et al., Inference and analysis of cell-cell communication using CellChat. Nat. Commun. 12, 1088 (2021).
85. S. Suo et al., Revealing the critical regulators of cell identity in the mouse cell atlas. Cell Rep. 25, 1436–1445.e3 (2018).
86. A. K. Westfall, Python single nucleus. Github. https://github.com/akwestfall/PythonSingleNucleus. Deposited 24 August 2023.
87. S. S. Gopalan et al., Python transcriptomics. NCBI BioProject. https://www.ncbi.nlm.nih.gov/bioproject/PRJNA1080230/. Deposited 25 February 2024.